Modulation of ECG Atrial Flutter Wave Amplitude by Heart Motion: A Model-based and a Bedside Estimate

V Jacquemet[1,2], B Dubé[2], P van Dam[3], AR LeBlanc[1,2], R Nadeau[2], M Sturmer[2], T Kus[1,2], A Vinet[1,2]

[1]Université de Montréal, Montréal, Canada
[2]Hôpital du Sacré-Coeur de Montréal, Montréal, Canada
[3]Peacs, Arnhem, The Netherlands

Abstract

This paper reports two attempts at estimating the magnitude of atrial flutter amplitude modulation caused by atrial motion during heart contraction. The first approach consists in analyzing the ECG of a patient in flutter with atrioventricular block and an implanted pacemaker. These conditions facilitate QRST cancellation, even in the presence of time-varying flutter wave amplitude. The second approach is based on a computer model of atrial flutter embedded in a torso model featuring predetermined motion of the atria. The results suggests that this lead-dependent effect is usually not large enough to preclude reasonably accurate QRST cancellation or T-wave extraction.

1. Introduction

During atrial arrhythmia, ventricular contraction may modulate the morphology of the atrial contribution to the ECG by moving or constraining atrial geometry and by affecting blood pressure. Ravelli et al. demonstrated that this effect can cause fluctuations in atrial cycle length [1, 2]. We hypothesized that ventricular contraction induces small changes in atrial signal amplitude on the thorax.

Our aim is to estimate an upper bound for this effect as it could affect the interpretation of QRST cancellation during atrial fibrillation and flutter. If ventricle-induced changes in atrial wave amplitude were large, they would limit the ability to predict atrial signal in the QT segment from data measured in the TQ segment [3]. QRST templates computed using average beat subtraction algorithms would also include some ventricular-contraction-dependent contribution from the atria.

Two approaches were investigated. The first estimate was based on ECG in a patient in which QRST cancellation was facilitated by the atria and the ventricles being activated independently and at a different rate. The second estimate was based on a simplified atrial model with time-dependent geometry embedded in a torso model.

2. Methods

2.1. Patient data

A patient in stable atrial flutter with complete atrioventricular block and a pacemaker was selected. Three-lead ECG was recorded during one hour at rest (Burdick Holter, Model 6632). Electrode configuration was designed to generate 3 pseudo-orthogonal leads X, Y and Z (X = V5 vs V6r; Y = upper sternal vs LL; Z = V3r vs V9). Sampling frequency was 500 Hz. All signals were band-pass filtered (0.01–100 Hz). During ECG recording, the pacemaker was programmed to deliver ventricular stimuli at a fixed rate of 40 bpm. As a result, the atria and the ventricles were both activated at a stable rate, but without any causal relation between atrial and ventricular activation.

2.2. Atrial signal extraction

Atrial and ventricular components of the ECG were separated using an average-beat subtraction method [4]. The n-th beat of a lead of the ECG, that is, the segment between the n-th and the $(n+1)$-th R wave, is written as

$$ECG_n(t) = A_n(t) + V_n(t)\ , \quad t \in [0, T_v] \qquad (1)$$

where A_n and V_n are respectively the atrial and the ventricular contribution, and T_v is the ventricular pacing cycle length. Since ventricular rate is fixed over a long period, the morphology of the QRST complex is expected to remain stable:

$$V_n(t) = v(t)\ , \quad t \in [0, T_v]\ . \qquad (2)$$

Assuming that the atrial signal is also stable with an amplitude possibly modulated by the phase in the ventricular cycle

$$A_n(t) = m(t) \cdot a(t - \tau_n)\ , \quad t \in [0, T_v]\ . \qquad (3)$$

where $m(t)$ is an amplitude modulation function, $a(t)$ is the atrial signal waveform (zero-mean periodic function of

period T_a), and τ_n is the time shift between atrial and ventricular activation at beat n.

The ECG averaged over N beats (after R-wave alignment) gives:

$$\overline{ECG}(t) = \frac{1}{N}\sum_n \Big(A_n(t) + V_n(t)\Big) \quad (4)$$

$$= v(t) + m(t)\frac{1}{N}\sum_n a(t-\tau_n) \quad (5)$$

If the time shift τ_n is uniformly distributed between 0 and T_a, the atrial contribution vanishes:

$$\frac{1}{N}\sum_n a(t-\tau_n) \approx \frac{1}{T_a}\int_0^{T_a} a(t-\tau)\mathrm{d}\tau = 0 \quad (6)$$

so that the ventricular component can recovered by averaging the ECG, i.e., $\overline{ECG}(t) = v(t)$. The atrial component is computed as $A_n(t) = ECG_n(t) - \overline{ECG}(t)$.

2.3. F-wave amplitude

The modulation function $m(t)$ may be identified by taking the maximum over all the beats:

$$\max_n A_n(t) = m(t)\max_n a(t-\tau_n) \approx m(t)\; a_{max}\;. \quad (7)$$

This is an appropriate method for simulated signals. Sensitivity to noise limits its applicability to clinical data.

To increase robustness, a min/max filter with window length of one flutter period was applied to $A_n(t)$ to compute the upper envelope $A_n^+(t)$ and lower envelope of the signal $A_n^-(t)$. F-wave amplitude was defined as $(A_n^+(t) - A_n^-(t))/2$. Mean and standard deviation (SD) of F-wave amplitude averaged over the beats were computed as a function of t (time from the R peak).

2.4. Modeling framework

The goal is to create a modeling environment to estimate the effect of heart motion on the atrial component of the ECG. In order to provide a worst-case estimate, simplifying hypotheses will be made:

- The torso is assumed to be motionless and with uniform conductivity. The subject is relatively lean, so the heart is close to the surface of the thorax.
- Respiration effects are not taken into account to isolate the contribution of heart motion.
- The movement of the atria will follow a prescribed transformation optimized for normal rhythm. This will overestimate the variations in volume and orientation when applied to macroreentrant atrial activity.
- Membrane currents are supposed to be unaffected by stretch or contraction.
- A simplified model of atrial propagation will be used (simplified geometry; uniform propagation).

2.5. Model geometry

Magnetic resonance image (MRI) acquisition was performed on a relatively lean, male healthy subject. Heart rate was 80 bpm (750 ms). Using R-wave gated synchronization, 50 time instants were recorded during the cardiac cycle (one image every 15 ms). Images were segmented. Atrial, ventricular and torso geometry was reconstructed as low-resolution triangular meshes. An atrial mesh was selected to create a higher-resolution higher-quality mesh appropriate for numerical methods (reference mesh). Rigid registration was applied by computing the optimal affine transform $f(\vec{y}) = A(t)\vec{y} + \vec{b}$ between the reference mesh ($\vec{y}_i$) and the atrial meshes corresponding to other time instants ($\vec{x}_j(t)$). The following error function

$$e^2(A,\vec{b};t) = \sum_i \min_j \|A(t)\vec{y}_i + \vec{b}(t) - \vec{x}_j(t)\|^2 \quad (8)$$

was minimized with respect to the 12 entries of the matrix A and the vector $\vec{b}$ for each of the 50 time instants. The MATLAB implementation of multidimensional unconstrained nonlinear minimization algorithm (Nelder-Mead) was used. Torso geometry was assumed to remain unchanged during the cardiac cycle.

2.6. Atrial activation

Flutter-like reentrant activation was simulated using the monodomain equations in a simplified atrial geometry with uniform conduction properties [5]. The evolution of the transmembrane potential V_m was governed by the reaction-diffusion equation:

$$C_m\,\frac{\partial V_m}{\partial t} = \beta^{-1}\,\nabla\cdot\sigma\,\nabla V_m - I_{ion} \quad (9)$$

where C_m is the membrane capacitance per unit area of membrane, β is the area of membrane per unit volume, and σ is the effective conductivity. No-flux boundary condition was assumed. The ionic current flowing through the membrane I_{ion} was described by the Courtemanche model of membrane kinetics [6]. L-type calcium current was inhibited by 75% to reduce action potential duration and rate adaptation and thus stabilize the reentry.

A cubic mesh (748,741 nodes, $\Delta x = 0.33$ mm, thickness $\approx$ 1.6 mm) was created to represent the atrial myocardium [5]. Parameters were set to $C_m = 1$ μF/cm^2, $\beta = 2000$ cm^{-1}, $\sigma = 4.2$ mS/cm. Monodomain equations were solved using finite-volume discretization and forward Euler numerical, assuming that the atrial geometry was fixed. A flutter-like reentrant activation was initiated using a programmed stimulation protocol [5]. Membrane currents $I_i(t)$ flowing into the extracellular medium (source current for the volume conduction problem) were

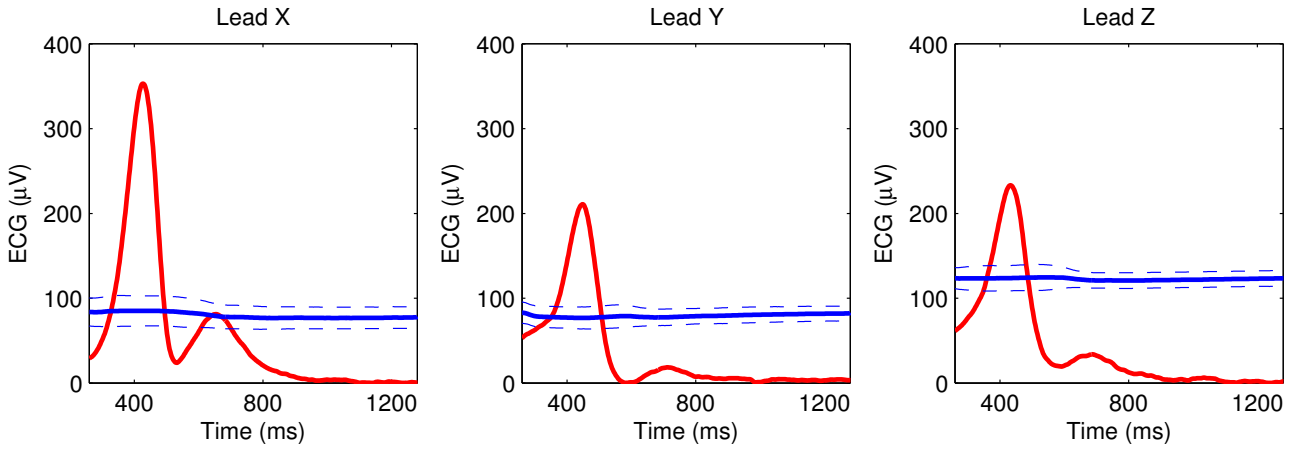

Figure 1. Amplitude of flutter waves extracted from patient data as a function of the time in the cardiac cycle (for each lead), mean (blue solid line) ± standard deviation (dashed lines). The T and U waves are shown for reference (red curves). RR interval (T_v) is 1500 ms and atrial cycle length (T_a) is 314 ms.

computed at each node i after 1 sec of stable reentrant activity.

2.7. ECG computation and analysis

ECGs were computed in a homogeneous torso with a two-step approach. First, the volume conduction medium was assumed to be homogeneous and unbounded. In this case, the potential at point $\vec{z}$ reads:

$$\phi_\infty(\vec{z},t;\tau) = \frac{1}{4\pi\sigma_e}\sum_i \frac{I_i(t-\tau)}{\|\vec{x}_i(t)-\vec{z}\|} \qquad (10)$$

where $I_i(t)$ is the membrane current flowing into the extracellular medium in the volume element located at $\vec{x}_i$ and σ_e is the extracellular conductivity. The parameter τ is the phase shift between atrial and ventricular electrical activity. It corresponds to the variable τ_n in clinical signals [Eq. (3)]. The potential ϕ_∞ is computed at each vertex of the mesh of the torso. Then, the effect of torso boundary is taken into account using boundary element methods [7]:

$$\phi(\vec{z},t) = 2\,\phi_\infty(\vec{z},t) - \frac{1}{2\pi}\int_S \phi(\vec{x},t)\,\mathrm{d}\Omega(\vec{x},\vec{z}) \qquad (11)$$

where S is the surface of the torso, $\mathrm{d}\Omega(\vec{x},\vec{z})$ is the solid angle subtended by the surface element located at $\vec{x}$ with respect to the point $\vec{z}$. As a result, the body surface potential ϕ is a linear combination of the potentials ϕ_∞.

Signals corresponding to the X, Y and Z leads were computed in the time interval $[0, T_v]$ for τ varying from 0 to T_a during simulated flutter-like activity. F-wave amplitude envelopes were extracted based on Eq. (7) where the maximum was taken over all possible values of τ.

3. Results

For patient data, the phase shift τ_n was computed from the position of the largest positive peak of the cross-correlation between flutter waves in the TQ interval of the first and the n-th beat. The distribution of intervals between R waves and flutter waves (τ_n) was not significantly different from a uniform distribution (p=0.28; Kolmogorov-Smirnov test). As a result, most of the atrial activity was suppressed by beat averaging, as illustrated in Fig. 1 (red curves). Note that the U wave was kept intact. Figure 1 shows that the amplitude of the envelope of F waves as a function of the time in the cardiac cycle remained relatively stable. Variations in average F-wave amplitude due to heart motion were of the order of background noise and fluctuations caused by breathing.

Figure 2 shows signals representing the atrial contribution to the simulated ECG computed using a moving heart geometry. The coefficient of variation (SD/mean) of the envelope of F-wave amplitudes during the cardiac cycle was 4.4%, 5.8% and 25% respectively for lead X, Y and Z. Larger variations in lead Z were due to the small distance between one of the electrode and the heart.

4. Discussion and conclusions

Modulation of atrial ECG morphology by heart motion might deteriorate the performance of QRST cancellation and T-wave extraction algorithms. In the clinical ECG, the effect was found to be small. However, the patient had pre-existing heart problems that necessitated pacemaker implantation. This patient may therefore correspond to a best-case scenario as far as QRST cancellation is concerned. The influence of heart motion is expected to be

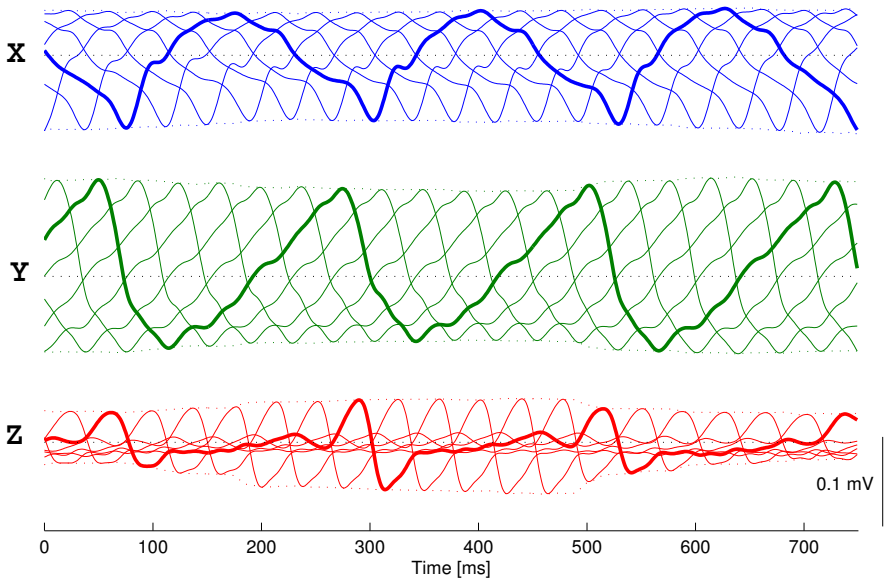

Figure 2. Simulation of the atrial contribution to pseudo-orthogonal ECGs (lead X, Y and Z) for different phase shifts between atrial and ventricular activation. One of the lines is thicker to emphasize signal morphology. Time from 0 to 750 ms represents a cardiac cycle from a R wave to the next one.

larger when the ventricles are healthier. Furthermore, uniform phase distribution is unlikely when ventricular activation is triggered by the atria.

The computer model was aimed at assessing the sensitivity of the forward problem during atrial flutter with respect to displacement of atrial geometry. Since atrial motion during normal rhythm was incorporated in the model, the geometrical effect is overestimated, thus providing a worst-case model. More sophisticated models [8] would need to be developed to accurately describe these effects and overcome the strong limitations listed in Subsect. 2.4. Our simplified model may still be used for the identification of electrode configurations that are least affected by heart motion.

Acknowledgements

This research is supported by the Natural Sciences and Engineering Research Council of Canada (NSERC) and Heart and Stroke Foundation of Quebec.

References

[1] Ravelli F, Mase M, Disertori M. Mechanical modulation of atrial flutter cycle length. Prog Biophys Mol Biol 2008;97(2-3):417–34.

[2] Mase M, Glass L, Ravelli F. A model for mechano-electrical feedback effects on atrial flutter i nterval variability. Bull Math Biol 2008;70(5):1326–47.

[3] Sassi R, Corino VDA, Mainardi LT. Analysis of surface atrial signals: time series with missing data? Ann Biomed Eng 2009;37(10):2082–92.

[4] Lemay M, Vesin JM, van Oosterom A, Jacquemet V, Kappenberger L. Cancellation of ventricular activity in the ECG: evaluation of novel and existing methods. IEEE Trans Biomed Eng 2007;54(3):542–6.

[5] Jacquemet V, van Oosterom A, Vesin JM, Kappenberger L. Analysis of electrocardiograms during atrial fibrillation. A biophysical model approach. IEEE Eng Med Biol Mag 2006; 25(6):79–88.

[6] Courtemanche M, Ramirez RJ, Nattel S. Ionic mechanisms underlying human atrial action potential properties: insights from a mathematical model. Am J Physiol 1998;275(1 Pt 2):H301–21.

[7] van Oosterom A, Jacquemet V. Genesis of the P wave: atrial signals as generated by the equivalent double layer source model. Europace 2005;7 Suppl 2:21–9.

[8] Wei Q, Liu F, Appleton B, Xia L, Liu N, Wilson S, Riley R, Strugnel W, Slaughter R, Denman R, Crozier S. Effect of cardiac motion on body surface electrocardiographic potentials: an MRI-based simulation study. Phys Med Biol 2006; 51(14):3405–18.

Address for correspondence:

Vincent Jacquemet
Hôpital du Sacré-Coeur de Montréal, Centre de Recherche
5400 boul. Gouin Ouest, Montréal (QC), Canada H4J 1C5
vincent.jacquemet@umontreal.ca